Sodium borohydride (NaBH 4) as a high-capacity material for next-generation sodium-ion capacitors

Pawel Jeżowski, Olivier Crosnier, Thierry Brousse

▶ **To cite this version:**

Pawel Jeżowski, Olivier Crosnier, Thierry Brousse. Sodium borohydride (NaBH 4) as a high-capacity material for next-generation sodium-ion capacitors. Open Chemistry, 2021, 19 (1), pp.432-441. ⟨10.1515/chem-2021-0040⟩. ⟨hal-03266196⟩

HAL Id: hal-03266196

https://hal.science/hal-03266196v1

Submitted on 18 Nov 2021

HAL is a multi-disciplinary open access archive for the deposit and dissemination of scientific research documents, whether they are published or not. The documents may come from teaching and research institutions in France or abroad, or from public or private research centers.

L'archive ouverte pluridisciplinaire **HAL**, est destinée au dépôt et à la diffusion de documents scientifiques de niveau recherche, publiés ou non, émanant des établissements d'enseignement et de recherche français ou étrangers, des laboratoires publics ou privés.

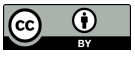

Distributed under a Creative Commons CC BY 4.0 - Attribution - International License

Research Article

Pawel Jeżowski*, Olivier Crosnier, Thierry Brousse

Sodium borohydride ($NaBH_4$) as a high-capacity material for next-generation sodium-ion capacitors

https://doi.org/10.1515/chem-2021-0040
received December 1, 2020; accepted March 8, 2021

Abstract: Energy storage is an integral part of the modern world. One of the newest and most interesting concepts is the internal hybridization achieved in metal-ion capacitors. In this study, for the first time we used sodium borohydride ($NaBH_4$) as a sacrificial material for the preparation of next-generation sodium-ion capacitors (NICs). $NaBH_4$ is a material with large irreversible capacity of ca. 700 mA h g^{-1} at very low extraction potential close to 2.4 vs Na^+/Na^0. An assembled NIC cell with the composite-positive electrode (activated carbon/$NaBH_4$) and hard carbon as the negative one operates in the voltage range from 2.2 to 3.8 V for 5,000 cycles and retains 92% of its initial capacitance. The presented NIC has good efficiency >98% and energy density of ca. 18 W h kg^{-1} at power 2 kW kg^{-1} which is more than the energy (7 W h kg^{-1} at 2 kW kg^{-1}) of an electrical double-layer capacitor (EDLC) operating at voltage 2.7 V with the equivalent components as in NIC. Tin phosphide (Sn_4P_3) as a negative electrode allowed the reaching of higher values of the specific energy density 33 W h kg^{-1} (ca. four times higher than EDLC) at the power density of 2 kW kg^{-1}, with only 1% of capacity loss upon 5,000 cycles and efficiency >99%.

Keywords: sodium-ion capacitors, sacrificial salt, sodium inorganic salt, pre-sodiation, composite carbon electrode

* **Corresponding author: Pawel Jeżowski,** Université de Nantes, CNRS, Institut des Matériaux Jean Rouxel, IMN, F-44000 Nantes, France; Réseau sur le Stockage Electrochimique de l'Energie (RS2E), CNRS FR 3459, 33 rue Saint Leu, 80039 Amiens, Cedex, France; Poznan University of Technology, Institute of Chemistry and Technical Electrochemistry, Berdychowo 4, 60-965, Poznań, Poland, e-mail: pawel.jezowski@put.poznan.pl
Olivier Crosnier, Thierry Brousse: Université de Nantes, CNRS, Institut des Matériaux Jean Rouxel, IMN, F-44000 Nantes, France; Réseau sur le Stockage Electrochimique de l'Energie (RS2E), CNRS FR 3459, 33 rue Saint Leu, 80039 Amiens, Cedex, France

1 Introduction

In the recent years, the topic of hybrid energy storage devices categorized as metal-ion capacitors (MICs) has been receiving the attention of scientists due to their high energy and power output [1–4]. MICs are constructed of a positive electrode, most often activated carbon (AC), which stores energy in the electrical double layer [5,6]. On the other side, the faradaic-negative electrode undergoes a reversible redox reaction of metal ions [7,8]. The biggest flaw of MICs is the necessary pre-insertion step of the negative electrode to form a fully functioning MIC. The biggest record of pre-insertion topics is related to the lithium-based devices called lithium-ion capacitors (LICs), where three techniques are used to this day:

(1) Use of metallic lithium:
The first method has two variations:
- Pre-insertion with metallic lithium can be done in two steps. First, the negative electrode undergoes a metal-ion intercalation in a cell with a metallic lithium as a second electrode. Second, the pre-lithiated-negative electrode is shifted to a second cell with an AC-positive electrode to form an operational LIC [9]. All manipulations are carried out under an inert atmosphere to limit the exposure of cell elements to O_2 or H_2O, which greatly increases the cost [10].
- One-step assembly can be achieved if an auxiliary lithium electrode is added during the cell construction. The graphite electrode is connected externally versus the metallic lithium electrode and once the pre-lithiation is finished, the connection is then swapped to graphite intercalation compound versus AC electrode [11,12]. There are two problems with this approach, the first being that the construction of the cell is very complex.

However, the biggest flaw of a metallic electrode used is the dendrite formation on its surface which can lead to cell short circuiting and thermal runaway [13–15].

Open Access. © 2021 Pawel Jeżowski *et al.*, published by De Gruyter. This work is licensed under the Creative Commons Attribution 4.0 International License.

(2) Use of lithium ions in the electrolyte

The second method incorporates in the cell construction a high-concentration lithium-ion electrolyte. However, the electrolyte conductivity decreases once the pre-insertion step is complete, which is considered an enormous drawback leading to worse electrochemical performance and shorter cyclability of the cell [16].

(3) Use of sacrificial material:

The third proposed method allows the assembly of LICs in one step, by using a sacrificial lithium source and AC in the form of a composite-positive electrode [17–22]. Lithium ions can be irreversibly extracted from the structure of the sacrificial material during initial oxidation. Extracted metal ions allow the concentration of lithium ions to stay at a constant value during the formation of the solid electrolyte interphase (SEI) and the intercalation of the negative electrode. The oxidized form of the sacrificial material after lithium ions are extracted can remain as electrochemically inactive "dead mass" in the composite-positive electrode [17,18] or can dissolve in the electrolyte [19]. The sacrificial material should fulfil one of the two main conditions: (1) a high irreversible capacity to reduce its amount in the positive electrode and (2) a low extraction potential to avoid electrolyte oxidation [17–22].

Lithium-based systems are expensive as lithium is one of the rarest elements on the Earth and its ores are located in geopolitically unstable regions. This is why we should lean towards the use of sodium and sodium-ion capacitors (NICs), which are starting to be promising energy storage devices [10]. The abundance of sodium is almost four orders of magnitude higher than lithium. Sodium ores are evenly distributed across the globe and are easily accessible in politically stable regions [23]. The most important advantages are (i) sodium does not form alloys with aluminium near the insertion potential, (ii) it is cheaper, and (iii) it is lighter than copper and could replace it in the near future [10]. The earliest work mentioning NIC is from 2012 by Kuratani et al. [24]. The mentioned work used a pre-sodiated hard carbon (HC)-negative electrode and an AC-positive electrode soaked in electrolyte; 1 mol L^{-1} $NaPF_6$ dissolved in ethylene carbonate (EC)/diethyl carbonate (DEC). Currently, the majority of the published studies present the use of a metallic sodium as a source of sodium ions for the pre-sodiation step to form a functional NIC [25–36]. Until now, there are only a few recent works that show the possible use of a sacrificial material; sodium sulphide (Na_2S) [37] or sodium amide ($NaNH_2$) [38]. However, once sodium is fully extracted from Na_2S, the positive electrode contains electrochemically inactive by-products such as polysulphides [39] from Na_2S oxidation. As this "dead mass" stays in the positive electrode, it can cause a reduction in the specific energy. Hence, it is necessary to search for materials which, after oxidation, would be liberated from the electrode material in gaseous form similar to the case of sodium amide.

In the search of such properties, sodium borohydride ($NaBH_4$) with a theoretical capacity of 670 mA h g^{-1} and possible formation gaseous by-products after oxidation seems to be a promising candidate for realizing the next-generation NICs with no dead mass. The results presented in this study confirms that all $NaBH_4$ is irreversibly extracted, while the BH_4^- anion is electrochemically oxidized and can be removed from the cell while not decreasing the specific energy and power of the NIC cell.

2 Methods and materials

2.1 Positive electrode preparation for NIC

In a glove box with less than 0.1 ppm of H_2O and O_2, 0.55 g of AC (Kuraray YP 80 F) and 0.25 g of $NaBH_4$ (Sigma Aldrich, 99.99%) were added to a round-bottom flask with 20 mL of *n*-heptane (anhydrous, ≥99%; Merck). The mixture was stirred using a magnetic stirrer.

Under the fume hood, 0.08 g of a 60% solution of binder polytetrafluoroethylene (PTFE, 60% dispersion in water; Merck) and 0.15 g of carbon black (Super C65, Imerys) were mixed in a beaker with 20 mL of ethanol using a magnetic stirrer at a rotational speed of 500 rpm and temperature of 90°C until the solvent is completely evaporated. The beaker was afterwards transferred to a vacuum oven at 120°C with continuous vacuum for 12 h to remove any residues of the solvent. The dried mixture in a beaker was then transferred to the glove box.

Once the dried mixture (PTFE and C65) was inside the glove box, it was added to a beaker with AC, $NaBH_4$, and 20 mL of *n*-heptane and mixed with a magnetic stirrer. The mixture was stirred until the excess solvent is evaporated and formation of dough-like matter from which a homogenous sheet of electrode material was formed (its thickness was about 140 μm). Electrodes with 16 mm diameter were cut with hollow punchers, then placed in a vial, dried in a glass oven B-585 vacuum drier at 120°C for 12 h, and then moved back to the glove box without contact with water or oxygen (to avoid any traces of moisture). Final composition of the composite-positive

electrode was 55 wt% of AC, 25 wt% of $NaBH_4$, 15 wt% of carbon black, and 5 wt% of PTFE. Mass of the electrode disk was about 7 mg cm^{-2}. For the experiments with tin phosphide, a negative electrode an additional batch of positive composite electrodes was prepared (their thickness was ca. 110 μm) and their composition was 45 wt% of AC, 35 wt% of $NaBH_4$, 15 wt% of carbon black, and 5 wt% of PTFE; and in this case, the mass of electrode disk was near 6 mg cm^{-2}.

2.2 Negative electrode preparation for NIC

The HC (Kureha grade, PJ, Japan) or tin phosphide (Sn_4P_3; referred to this article as SnP) was used for the preparation of two separate batches of negative electrodes. HC electrodes were prepared by mixing 0.91 g of HC (Kureha PJ), 1.6 g of PVDF solution dispersed in 1-methyl-2-pyrrolidinone (using a 5 wt% PVDF solution in NMP; 99.5% anhydrous, Sigma Aldrich), and 0.01 g of Super C65 with a homogenizer at 15,000 rpm for 15 min. An additional amount of 1 mL of NMP was introduced while mixing to decrease the ink viscosity. The final composition of the HC-negative electrode was 91 wt% of HC, 8 wt% of binder, and 1 wt% of soot. Then, the ink was laid out on aluminium foil (thickness 35 μm) by an automatic film applicator (thickness of the ink was set to be about 100 μm). NMP was evacuated from the coating by heating it to 100°C under a fume hood and further under vacuum at 120°C for 12 h. After drying, the coated foil was calendered with a laboratory roll press heated up to 70°C until reaching a thickness of approximately 90 μm, to improve the electrode material density and have contact with the current collector. Electrodes with a diameter of 16 mm were punched out from the calendered electrode sheet using a precision disc cutter. The mass loading of the HC electrode material was approximately 6 mg cm^{-2}. The Sn_4P_3 and the electrodes were prepared according to the detailed description reported elsewhere [36]. The mass loading of the electrode material was approximately 3 mg cm^{-2}.

2.3 Preparation of electrodes for electrical double-layer capacitor (EDLC)

To compare the energy and power densities under similar conditions, an EDLC cell was assembled with two AC electrodes prepared in ambient conditions. A mixture consisting of AC; 0.80 g (Kuraray YP80F), binder solution; 0.08 g (PTFE, 60% dispersion in water, Sigma Aldrich) and soot; 0.15 g (Super C65, Imerys) was mixed in a beaker with 20 mL of ethanol. The EDLC electrodes' final composition was 80 wt% of AC, 15 wt% of soot, and 5 wt% of binder. The mass loading of the electrode material was approximately 5 mg cm^{-2}.

2.4 Electrochemical investigation

All cells were assembled in an argon-filled glove box. For sodium extraction investigations, two-electrode cells were used (El-Cell, Germany). The cell was composed of a working electrode ($NaBH_4$/AC) and a counter/reference electrode (sodium disk of thickness ca. 250 μm). Both electrodes were separated from each other by a 670-μm thick GF/D Whatman membrane (diameter 18 mm), which was soaked with 450 μL of electrolyte 1 mol L^{-1} solution of sodium perchlorate ($NaClO_4$; Sigma Aldrich, >98%) dissolved in a mixture of EC and propylene carbonate (EC:PC, volumetric ratio 1:1, referred to as electrolyte throughout this study). The electrochemical process of sodium extraction from the $NaBH_4$/AC electrode was studied by cyclic voltammetry (CV) and galvanostatic charge/discharge with potential limitation (GCPL). In the case of CVs, the electrode potential was scanned from open circuit potential (OCP) to 4.0 V and backward to 2.0 V Na^+/Na^0 at a sweeping rate of 0.06 mV s^{-1}. GCPL on the Na_2BCN/AC composite-positive electrode was done at C/20 (where C corresponds to the theoretical capacity of $NaBH_4$, 670 mA h g^{-1}), and the potential range was the same as for the CV investigation.

A similar procedure was used for the investigation of negative electrode materials for NIC cells: HC or SnP. To establish the practical capacity of the HC electrode, the electrochemical reaction between sodium ions and HC electrode was performed by GCPL at a current density of 20 mA g^{-1}, starting from OCP until reaching a potential limitation of 5 mV vs Na^0/Na^+ (for HC) or 100 mV vs Na^+/Na^0 (for SnP) after which the sodium ions were deinserted until reaching 2.0 V vs Na^+/Na^0. The estimated initial capacity of the HC was ca. 300 mA h g^{-1} and SnP ca. 650 mA h g^{-1}.

The change in pressure during the electrochemical oxidation of $NaBH_4$ sacrificial was observed in ECC-Press-Air-DL (El-Cell).

The *in situ* X-ray diffraction (XRD) experiment was performed in the same cell and using the analogical methodology as described elsewhere [18].

The NICs were formed in a three-electrode cell from El-Cell. Positive ($NaBH_4$/AC) and negative electrodes

(HC or SnP) were separated by a porous membrane (El-Cell, thickness 1,550 µm) and soaked with electrolyte. A sodium pin was used as the reference electrode to monitor the potential of both electrodes. The reference electrode had only direct contact with the separator and was located at the same distance from the positive and negative electrodes. Mass ratio between AC and negative electrode active material was 1:1.

Pre-sodiation of the negative electrodes was achieved by GCPL at C/20 rate, starting from OCP until reaching a potential limitation for the positive electrode (4.0 V vs Na^+/Na^0) or 5 mV vs Na^+/Na^0 for HC and 100 mV for SnP vs Na^+/Na^0-negative electrode. After pre-sodiation, the NIC cells were conditioned for a total number of 300 cycles. Once the the cells are conditioned, the NIC cells were cycled for 5,000 cycles at one value of current density (125 mA g^{-1} for NIC cells with HC-negative electrode and 250 mA g^{-1} for NIC with SnP-negative electrode).

The EDLCs were assembled in two-electrode El-Cell cells. Positive and negative electrodes were composed of AC used in NIC cells and they had similar masses. Both electrodes were separated by a porous membrane (GF/D, Whatman, thickness 670 µm) soaked with 450 µL of electrolyte. The EDLC cells were conditioned by 300 cycles of CVs in the voltage range from 0.0 to 2.7 V at scanning rate of 5 mV s^{-1}. The specific energy of the cell was determined by the constant power method for both systems to avoid overestimation of achievable values in the case of EDLCs [40].

The electrochemical tests were done with a multichannel potentiostat/galvanostat with impedance channels (VMP3, Biologic), and the data were collected by EC-Lab v.11.32 software. Throughout the entire article, the values of specific capacitance, energy, and power are expressed per total mass of both electrodes for EDLC and NIC cells.

Ethical approval: The conducted research is not related to either human or animal use.

3 Results and discussion

The irreversibility of sodium extraction from $NaBH_4$ was analysed in a cell with a metallic sodium counter/reference electrode by cyclic voltamperometry and galvanostatic charge/discharge. The initial CV cycle (Figure 1a) shows an increase in anodic current corresponding to the sodium extraction process, and it starts to rise near 2.4 V vs Na^+/Na^0 and presents a maximum near 2.7 V vs Na^+/Na^0. However, during the cathodic sweep, no current response was observed, which means that the sodium extraction process is irreversible. Moreover, the following cycle (black solid line) displays a capacitive behaviour of AC, which is a major part of the composite electrode (Figure 1a). The galvanostatic charge/discharge at C/20 (where C corresponds to the theoretical capacity of $NaBH_4$, 710 mA h g^{-1}) in the potential range from 2.0 to 4.0 V vs Na^+/Na^0 (Figure 1b) shows a well-visible oxidation plateau at about 2.4 V vs Na^+/Na^0, and the absence of a plateau during negative polarization again confirms the irreversible character of the process. The practical irreversible capacity of sodium extraction is close to 700 mA h g^{-1}.

To confirm that the $NaBH_4$ is removed from the composition of the positive electrode, we performed separately two experiments: the *in situ* XRD (Figure 2a and b) and the *in operando* observation of pressure change during the polarization of the electrode (Figure 3a and b).

Upon the galvanostatic intermittent titration technique, which is composed of 1 h polarization periods at current C/20 (where C corresponds to the theoretical

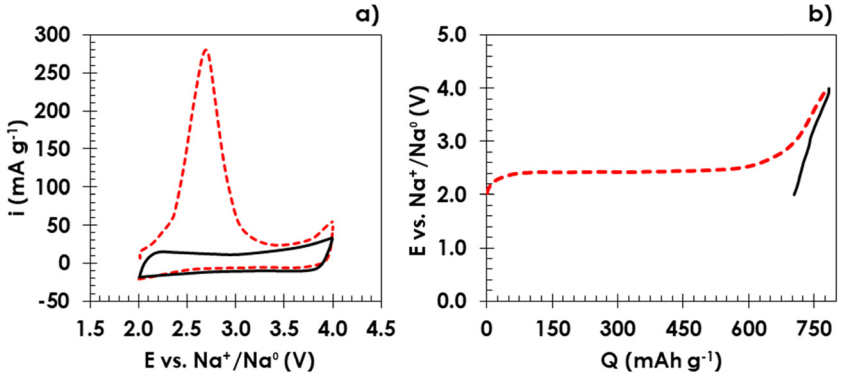

Figure 1: Electrochemical performance of the $NaBH_4$/AC composite electrode versus metallic sodium counter/reference electrode in the electrolyte: (a) cyclic voltamperometry at 0.06 mV s^{-1} (1st cycle: red dashed line; 2nd cycle: black solid line); (b) galvanostatic charge/discharge at C/20 up to 4.0 V vs N^+/Na^0 (charge: red dashed line; discharge: black solid line).

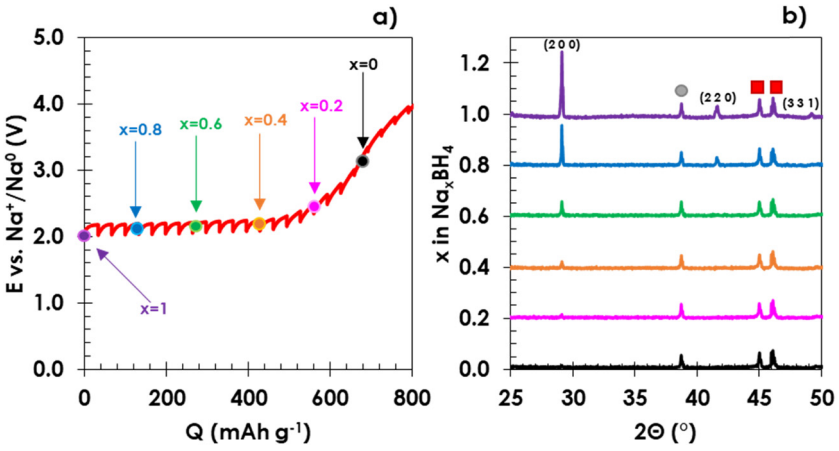

Figure 2: Electrochemical investigation and structural changes in $NaBH_4$: (a) galvanostatic intermittent titration technique with 1 h current pulse at current C/20 and 1 h OCV (during OCV period, the XRD spectra were taken); (b) structural changes in $NaBH_4$ presented as XRD spectra observed during the process of sodium extraction.

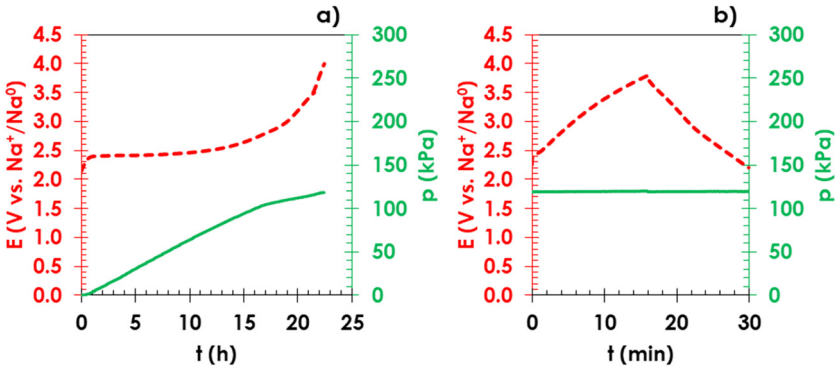

Figure 3: Galvanostatic oxidation of (a) $NaBH_4$ (red dashed line) and gas pressure measurement (green continuous line) and (b) charge/discharge profile of the positive electrode after the completion of $NaBH_4$oxidation.

capacity of $NaBH_4$) separated by 1 h OCV periods (Figure 2a) during which the XRD spectra were acquired (Figure 2b). It is presented that there is a visible disappearance of the signals corresponding to the cubic phase of $NaBH_4$ (marked with Miller indices at about 29, 42, and 49°) presence when the amount of sodium atoms are electrochemically removed from the structure of Na_xBH_4 ($x \to 0$, where x corresponds to the amount of sodium atoms). The only remaining signals after the complete extraction of sodium ions are related to the cell construction and they correspond to the aluminium current collector (grey circle, near 39°) and a beryllium window (red squares, near 45° and 46°).

To measure a pressure change during the polarization of $NaBH_4$/AC, an electrode cell with a pressure sensor was used. According to the manufacturer, the inner volume of this system is 4.45 cm^3. Figure 3a shows the profile of gas evolution (solid green line) and the galvanostatic polarization profile of the $NaBH_4$/AC (dashed red line) during the electrochemical sodium extraction. The investigated electrode had an initial mass of 15 mg, and it contained 3.5 mg (9.3×10^{-5} mol) of $NaBH_4$. The pressure change at 298 K related to BH_4^- oxidation was Δp = 112 kPa after 20 h of polarization. Hence, by application of the ideal gas law equation (1), one can calculate the total number of moles of produced gas:

$$n = \frac{p \times V}{R \times T} = \frac{112 \times 10^3 \times 4.45 \times 10^{-6}}{8.314 \times 298} = 2.01 \times 10^{-4} \text{ mol} \quad (1)$$

If the decomposition reaction follows equation (2) [41]:

$$NaBH_4 \rightarrow Na + B + \uparrow 2H_2 \quad (2)$$

the amount of gas produced should be 1.85×10^{-4} mol (starting from the initial 9.3×10^{-5} mol of $NaBH_4$); and as it is presented in equation (1), the gas production is 2.01×10^{-4} mol, which is the closest to the theoretical data. After the completion of electrochemical oxidation of $NaBH_4$, the positive electrode was again polarized (red dashed curve), with no additional charge of the internal pressure in the cell (Figure 3b).

Knowing the practical capacity of $NaBH_4$ (700 mA h g^{-1}), HC (300 mA h g^{-1} at cut-off potential 5 mV vs Na^+/Na^0), and tin phosphide (650 mA h g^{-1} at cut-off potential 0.1 V vs Na^+/Na^0), the composition of the positive electrode was estimated according to the calculation reported elsewhere [19]. In both cases of NICs, the mass ratio between the AC in the positive electrode and the active material in the negative electrode was equal to 1. In a cell with $NaBH_4$/AC-positive electrode and HC or SnP as the negative electrode, there was a sodium pin reference electrode, and it was possible to monitor the electrode potential during the formation of NIC. Potential limits were imposed as follows: 4 V for the positive electrode, 5 mV for HC electrode, or 100 mV for SnP vs Na^+/Na^0 to avoid any side reactions, such as electrolyte oxidation or sodium plating [19,42], or in the case of SnP to achieve the optimal electrochemical performance [36]. The pre-sodiation step was set at C/20 rate, where C corresponds to the practical capacity reached at the cut-off potential of HC (300 mA h g^{-1} at 5 mV vs Na^+/Na^0) or tin phosphide (650 mA h g^{-1} at 100 mV vs Na^+/Na^0). Figure 4a and c displays the potential profiles of electrodes and cell voltage during the formation of NIC. The sodium extraction from the $NaBH_4$/AC-positive electrode is characterized by one well-defined plateau at a potential near 2.4 V vs Na^+/Na^0 (red dashed line). The potential profile of sodium insertion (blue dotted line) in both cases drops drastically to 1.0 V Na^+/Na^0 below which SEI formation occurs together with specific adsorption of sodium ions down to potential of ca. 0.1 V vs Na^+/Na^0 for HC [36,37,42] and

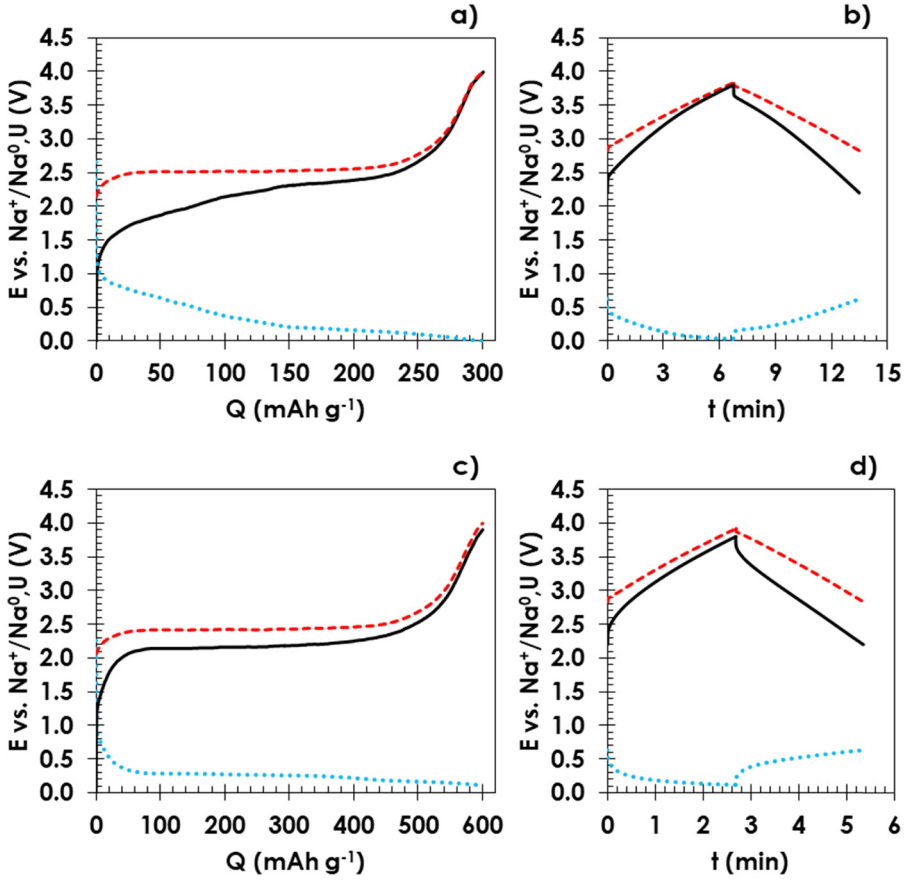

Figure 4: Pre-sodiation of a negative electrode (a) hard carbon, and (c) tin phosphide in an NIC with $NaBH_4$/AC-positive electrode. Galvanostatic profiles of the composite-positive electrode (red dashed line), -negative electrode (blue dotted line), and voltage of the cell (black solid line). Galvanostatic charge/discharge profiles of NIC with (b) HC-negative electrode at 125 mA g^{-1} and with (d) SnP-negative electrode at 250 mA g^{-1} (values given per gram of the total mass of the electrodes) in the voltage range 2.2–3.8 V.

0.2 V vs Na^+/Na^0 for SnP. Then the plateau formation is seen which corresponds to the insertion of sodium ions for HC and the formation of alloy for SnP [36,37]. The voltage profile of the full cell (black solid line) is the potential difference between the positive and negative electrodes. After pre-sodiation and conditioning, the NIC cells were cycled in the voltage range from 2.2 to 3.8 V. The NIC cell with HC-negative electrode (Figure 4b) was cycled at the current density of 125 mA g^{-1} and NIC with SnP-negative electrode (Figure 4d) was cycled at the current density of 250 mA g^{-1} (values of current density are presented per total mass of electrodes). The potential of the positive composite electrode (red dashed line) does not reach values lower than 2.0 V or higher than 4.1 V vs Na^+/Na^0, to avoid possible SEI formation on the surface of AC or electrolyte oxidation, respectively [36,37,42]. The lowest value of potential was 3 mV vs Na^+/Na^0 at the current density of 125 mA g^{-1}. For the NIC with SnP-negative electrode, the lowest reached value of potential by the negative electrode was 111 mV at the current density of 250 mA g^{-1}.

The dependence of specific capacitance (expressed per total mass of electrodes) versus the cycle number is shown in Figure 5a (NIC with HC-negative electrode) and Figure 5b (NIC with SnP-negative electrode). Both NICs were cycled in the voltage range of 2.2–3.8 V; but for NIC with HC-negative electrode, the current density was 125 mA g^{-1}; and for NIC with SnP-negative electrode, the current density was 250 mA g^{-1}. During galvanostatic cycling of NIC with HC-negative electrode at 125 mA g^{-1}, the NIC demonstrated a slow capacitance decrease during 5,000 cycles (Figure 5a) with a final 9% loss of capacitance in comparison with the initial value. While the NIC cells with SnP-negative electrode cycled at 250 mA g^{-1} displayed almost unchanged values of capacitance during the 5,000 cycles (Figure 5b) and the capacitance value dropped only by 1%.

Energy and power are characteristics of the assembled energy storage devices presented in Figure 6 as a Ragone plot. NICs were tested in the voltage from 2.2 to 3.8 V. A symmetric EDLC with the electrodes made of the same AC as the one used in the NIC impregnated with the

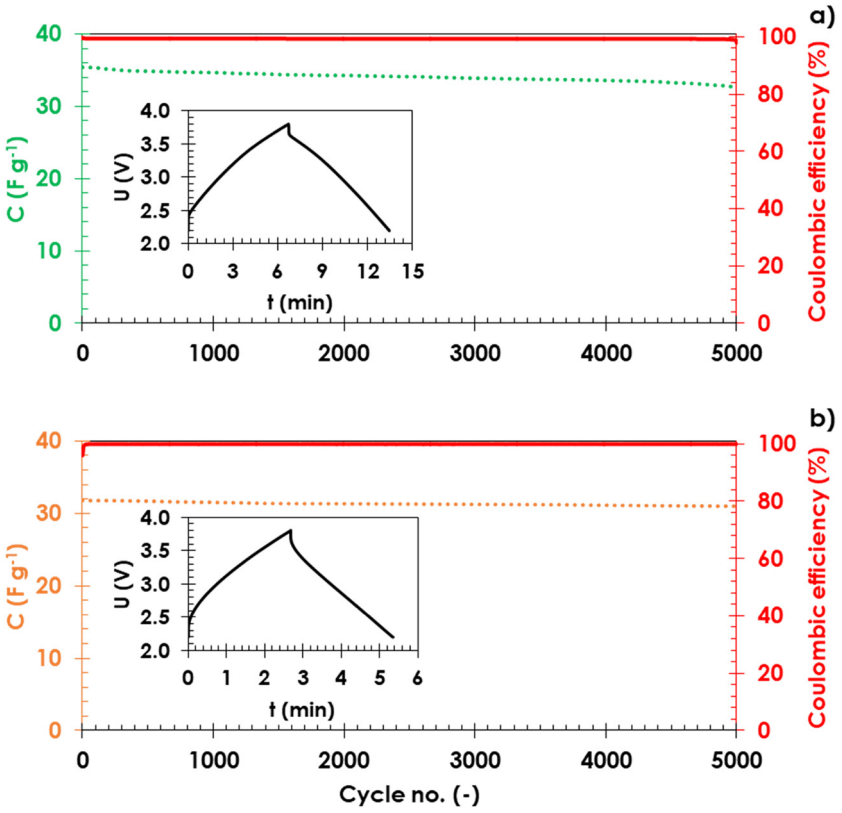

Figure 5: Specific capacitance of NIC with (a) hard carbon or (b) tin phosphide-negative electrode versus cycle number. Cells were galvanostatically charged/discharged in the voltage range of 2.2–3.8 V for 5,000 cycles at the current density (a) 125 mA g^{-1} or (b) 250 mA g^{-1}.

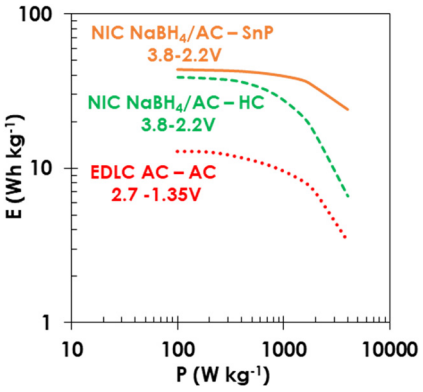

Figure 6: Ragone plots of the NICs prepared with NaBH$_4$/AC composite-positive electrode and hard carbon (green dashed line) or tin phosphide (orange solid line) in the voltage range of 2.2–3.8 V. For comparison, the EDLC cell data are presented (red dotted line) using the same AC as the electrode material, i.e. electrolyte as in NICs and charged up to 2.7 V.

same electrolyte was examined in the voltage range of 1.35–2.7 V [40]. Presented values are expressed per total mass of the electrodes. Calculated values of the energy density for the NICs are around 40 W h kg^{-1} at power values below 0.5 kW kg^{-1}, which is almost four times higher than in the case of the EDLCs (red dotted line) with organic electrolytes, where the values of energy are around 11 W h kg^{-1}. Moreover, the NIC with SnP-negative electrode (orange solid line) has superior electrochemical performance in comparison with the NIC with HC electrode (green dashed line). As it is presented in Figure 6, NIC with SnP-negative electrode maintains the best retention of energy value of about 33 W h kg^{-1} at power 2 kW kg^{-1}, while the energy density for the NIC with HC-negative electrode was lower, i.e. ca. 18 W h kg^{-1}; for comparison, the energy density for EDLC cells at the same power was ca. 6 W h kg^{-1}.

In comparison with other NICs reported so far with an HC-negative electrode, our cells achieved a longer cycle life than the one presented by Kuratani et al. [24]. Nevertheless, the potential of sodium insertion in HC is very low (near 5 mV vs Na^0/Na$^+$), which can contribute to sodium plating at higher current densities. Tin-based metallic anodes have a great advantage due to the high capacity, even 850 mA h g^{-1}; however, without a suitable buffer matrix to adsorb the volume changes in the active material during metal insertion/deinsertion, they show very poor cycle life [43,44]. Sn_4P_3 alloy proves so far to be one of the better materials for the negative electrode for a hybrid capacitor, and it demonstrates great improvement as the achievable energy reaches 33 W h kg^{-1} at 2 kW kg^{-1}, i.e. excellent capacitance retention after 5,000 cycles (99%).

4 Conclusion

Presented NICs used a sacrificial salt NaBH$_4$, which has not been so far reported in the literature as a source of sodium ions for pre-sodiation of the negative electrodes demonstrated to have a number of advantages. First, the extraction of sodium ions from NaBH$_4$ is completely irreversible and at the lowest potential 2.4 V Na^0/Na$^+$ reported so far. Additionally, the high irreversible capacity of 700 mA h g^{-1} leads to the reduction in the sacrificial material in the positive composite electrode to 25–35 wt%. Second, the cycling performance of the NIC system is stable and the NICs can work for 5,000 cycles. Last, what is most important, the operational voltage of this system is high enough to achieve reasonable energy and power output, reaching 33 W h kg^{-1} at 2 kW kg^{-1} in comparison with the conventional EDLCs.

Funding information: The authors are pleased to acknowledge the support of the Polish National Agency for Academic Exchange in funding under the Bekker programme, research stay and realization of NOVMAT project (PPN/BEK/2018/1/00123/DEC/1). O.C. and T.B. would like to acknowledge the French National Research Agency (STORE-EX Labex Project ANR-10-LABX-76-01).

Author contributions: P. J. was involved in conceptualization, data curation, methodology, resources, investigation, visualization, writing of the original draft; P. J. and O. C. contributed to formal analysis and project administration; and P. J., O. C., and T. B. were in charge of funding acquisition, validation, writing, review, and editing.

Conflict of interest: Pawel Jeżowski, who is the co-author of this article, is the current Editorial Board member of Open Chemistry. This fact did not affect the peer-review process. The authors declare no other conflicts of interest.

Data availability statement: The data sets generated during and/or analysed during the current study are available from the corresponding author on reasonable request.

References

[1] Du Pasquier A, Plitz I, Menocal S, Amatucci G. A comparative study of Li-ion battery, supercapacitor and nonaqueous asymmetric hybrid devices for automotive applications. J Power Sources. 2003;115:171–8. doi: 10.1016/S0378-7753(02)00718-8.

[2] Naoi K, Ishimoto S, Isobe Y, Aoyagi S. High-rate nano-crystalline $Li_4Ti_5O_{12}$ attached on carbon nano-fibers for hybrid supercapacitors. J Power Sources. 2010;195:6250–4. doi: 10.1016/j.jpowsour.2009.12.104.

[3] Béguin F, Frąckowiak E, editors. Supercapacitors: materials, systems, and applications. Weinheim, Germany: Wiley-VCH; 2013.

[4] Brousse T, Marchand R, Taberna P-L, Simon P. TiO_2 (B)/activated carbon non-aqueous hybrid system for energy storage. J Power Sources. 2006;158:571–7. doi: 10.1016/j.jpowsour.2005.09.020.

[5] Gorska B, Bujewska P, Fic K. Thiocyanates as attractive redox-active electrolytes for high-energy and environmentally-friendly electrochemical capacitors. Phys Chem Chem Phys. 2017;19:7923–35. doi: 10.1039/C7CP00722A.

[6] Jeżowski P, Kowalczewski PŁ. Starch as a green binder for the formulation of conducting glue in supercapacitors. Polymers. 2019;11:1648. doi: 10.3390/polym11101648.

[7] Kerr JB. Advances in lithium-ion batteries edited by Walter A. van Schalkwijk (University of Washington, Seattle) and Bruno Scrosati (University of Rome, "La Sapienza"). New York: Kluwer Academic/Plenum Publishers; 2002. x + 514 pp. $120.00. ISBN 0-306-47356-9; J Am Chem Soc. 2003;125:3670–1. doi: 10.1021/ja025282c.

[8] Schroeder M, Winter M, Passerini S, Balducci A. On the cycling stability of lithium-ion capacitors containing soft carbon as anodic material. J Power Sources. 2013;238:388–94. doi: 10.1016/j.jpowsour.2013.04.045.

[9] Aida T, Murayama I, Yamada K, Morita M. Improvement in cycle performance of a high-voltage hybrid electrochemical capacitor. Electrochem Solid-State Lett. 2007;10:A93. doi: 10.1149/1.2435511.

[10] Ding J, Hu W, Paek E, Mitlin D. Review of hybrid ion capacitors: from aqueous to lithium to sodium. Chem Rev. 2018;118:6457–98. doi: 10.1021/acs.chemrev.8b00116.

[11] (a) Ando N, Kojima K, Tasaki S, Taguchi H, Fujii T, Hato Y, et al. Organic electrolyte capacitor, US2007/0002524A1; 2007; (b) Tanizaki H, Ando N, Hato Y. Lithium-ion capacit, EP1914764A1; 2007.

[12] (a) Naoshi Y, Takashi C, Kazuyoshi O, Kuniyasu H. Lithium-ion capacitor, WO2012063545A1; 2012; (b) Makoto T, Chiaki M. Lithium-ion capacit, JP2009059732A; 2009.

[13] Aurbach D. A short review of failure mechanisms of lithium metal and lithiated graphite anodes in liquid electrolyte solutions. Solid State Ion. 2002;148:405–16. doi: 10.1016/S0167-2738(02)00080-2.

[14] Luo W, Zhou L, Fu K, Yang Z, Wan J, Manno M, et al. A thermally conductive separator for stable Li metal anodes. Nano Lett. 2015;15:6149–54. doi: 10.1021/acs.nanolett.5b02432.

[15] Goodenough JB, Kim Y. Challenges for rechargeable Li batteries. Chem Mater. 2010;22:587–603. doi: 10.1021/cm901452z.

[16] Decaux C, Lota G, Raymundo-Piñero E, Frackowiak E, Béguin F. Electrochemical performance of a hybrid lithium-ion capacitor with a graphite anode preloaded from lithium bis(trifluoromethane)sulfonimide-based electrolyte. Electrochim Acta. 2012;86:282–6. doi: 10.1016/j.electacta.2012.05.111.

[17] Jeżowski P, Fic K, Crosnier O, Brousse T, Béguin F. Use of sacrificial lithium nickel oxide for loading graphitic anode in Li-ion capacitors. Electrochim Acta. 2016;206:440–5. doi: 10.1016/j.electacta.2015.12.034.

[18] Jeżowski P, Fic K, Crosnier O, Brousse T, Béguin F. Lithium rhenium(VII) oxide as a novel material for graphite pre-lithiation in high performance lithium-ion capacitors. J Mater Chem A. 2016;4:12609–15. doi: 10.1039/C6TA03810G.

[19] Jeżowski P, Crosnier O, Deunf E, Poizot P, Béguin F, Brousse T. Safe and recyclable lithium-ion capacitors using sacrificial organic lithium salt. Nat Mater. 2018;17:167–73. doi: 10.1038/nmat5029.

[20] Park M-S, Lim Y-G, Park J-W, Kim J-S, Lee J-W, Kim JH, et al. Li_2RuO_3 as an additive for high-energy lithium-ion capacitors. J Phys Chem C. 2013;117:11471–8. doi: 10.1021/jp4005828.

[21] Park M-S, Lim Y-G, Hwang SM, Kim JH, Kim J-S, Dou SX, et al. Scalable integration of Li_5FeO_4 towards robust, high-performance lithium-ion hybrid capacitors. ChemSusChem. 2014;7:3138–44. doi: 10.1002/cssc.201402397.

[22] Lim Y-G, Kim D, Lim J-M, Kim J-S, Yu J-S, Kim Y-J, et al. Anti-fluorite Li_6CoO_4 as an alternative lithium source for lithium ion capacitors: an experimental and first principles study. J Mater Chem A. 2015;3:12377–85. doi: 10.1039/C5TA00297D.

[23] Rumble J, editor. Handbook of chemistry and physics. Boca Raton, FL: CRC Press; 2020.

[24] Kuratani K, Yao M, Senoh H, Takeichi N, Sakai T, Kiyobayashi T. Na-ion capacitor using sodium pre-doped hard carbon and activated carbon. Electrochim Acta. 2012;76:320–5. doi: 10.1016/j.electacta.2012.05.040.

[25] Ajuria J, Redondo E, Arnaiz M, Mysyk R, Rojo T, Goikolea E. Lithium and sodium ion capacitors with high energy and power densities based on carbons from recycled olive pits. J Power Sources. 2017;359:17–26. doi: 10.1016/j.jpowsour.2017.04.107.

[26] Ding R, Qi L, Wang H. An investigation of spinel $NiCo_2O_4$ as anode for Na-ion capacitors. Electrochim Acta. 2013;114:726–35. doi: 10.1016/j.electacta.2013.10.113.

[27] Chen Z, Augustyn V, Jia X, Xiao Q, Dunn B, Lu Y. High-performance sodium-ion pseudocapacitors based on hierarchically porous nanowire composites. ACS Nano. 2012;6:4319–27. doi: 10.1021/nn300920e.

[28] Kurra N, Alhabeb M, Maleski K, Wang C-H, Alshareef HN, Gogotsi Y. Bistacked titanium carbide (MXene) anodes for hybrid sodium-ion capacitors. ACS Energy Lett. 2018;3:2094–100. doi: 10.1021/acsenergylett.8b01062.

[29] Kim MS, Lim E, Kim S, Jo C, Chun J, Lee J. General synthesis of N-doped macroporous graphene-encapsulated mesoporous metal oxides and their application as new anode materials for sodium-ion hybrid supercapacitors. Adv Funct Mater. 2017;27:1603921. doi: 10.1002/adfm.201603921.

[30] Dong J, Jiang Y, Li Q, Wei Q, Yang W, Tan S, et al. Pseudocapacitive titanium oxynitride mesoporous nanowires with iso-oriented nanocrystals for ultrahigh-rate sodium ion hybrid capacitors. J Mater Chem A. 2017;5:10827–35. doi: 10.1039/C7TA00463J.

[31] Tong Z, Liu S, Zhou Y, Zhao J, Wu Y, Wang Y, et al. Rapid redox kinetics in uniform sandwich-structured mesoporous Nb_2O_5/graphene/mesoporous Nb_2O_5 nanosheets for high-performance sodium-ion supercapacitors. Energy Storage Mater. 2018;13:223–32. doi: 10.1016/j.ensm.2017.12.005.

[32] Zhu Y-E, Yang L, Sheng J, Chen Y, Gu H, Wei J, et al. Fast Sodium storage in TiO_2@CNT@C nanorods for high-performance Na-ion capacitors. Adv Energy Mater. 2017;7:1701222. doi: 10.1002/aenm.201701222.
[33] Gu H, Kong L, Cui H, Zhou X, Xie Z, Zhou Z. Fabricating high-performance sodium ion capacitors with P2-$Na_{0.67}Co_{0.5}Mn_{0.5}O_2$ and MOF-derived carbon. J Energy Chem. 2019;28:79–84. doi: 10.1016/j.jechem.2018.01.012.
[34] Le Z, Liu F, Nie P, Li X, Liu X, Bian Z, et al. Pseudocapacitive sodium storage in mesoporous single-crystal-like TiO_2 – graphene nanocomposite enables high-performance sodium-ion capacitors. ACS Nano. 2017;11:2952–60. doi: 10.1021/acsnano.6b08332.
[35] Dong S, Shen L, Li H, Pang G, Dou H, Zhang X. Flexible sodium-ion pseudocapacitors based on 3D $Na_2Ti_3O_7$ nanosheet arrays/carbon textiles anodes. Adv Funct Mater. 2016;26:3703–10. doi: 10.1002/adfm.201600264.
[36] Chojnacka A, Pan X, Jeżowski P, Béguin F. High performance hybrid sodium-ion capacitor with tin phosphide used as battery-type negative electrode. Energy Storage Mater. 2019;22:200–6. doi: 10.1016/j.ensm.2019.07.016.
[37] Pan X, Chojnacka A, Jeżowski P, Béguin F. Na_2S sacrificial cathodic material for high performance sodium-ion capacitors. Electrochim Acta. 2019;318:471–8. doi: 10.1016/j.electacta.2019.06.086.
[38] Jeżowski P, Chojnacka A, Pan X, Béguin F. Sodium amide as a "zero dead mass" sacrificial material for the pre-sodiation of the negative electrode in sodium-ion capacitors. 2021;375:137980. doi: 10.1016/j.electacta.2021.137980.
[39] Wang L, Zhang T, Yang S, Cheng F, Liang J, Chen J. A quantum-chemical study on the discharge reaction mechanism of lithium-sulfur batteries. J Energy Chem. 2013;22:72–7. doi: 10.1016/S2095-4956(13)60009-1.
[40] Zhao J, Gao Y, Burke AF. Performance testing of super-capacitors: important issues and uncertainties. J Power Sources. 2017;363:327–40. doi: 10.1016/j.jpowsour.2017.07.066.
[41] Urgnani J, Torres FJ, Palumbo M, Baricco M. Hydrogen release from solid state $NaBH_4$. Int J Hydrog Energy. 2008;33:3111–5. doi: 10.1016/j.ijhydene.2008.03.031.
[42] Cao WJ, Zheng JP. Li-ion capacitors with carbon cathode and hard carbon/stabilized lithium metal powder anode electrodes. J Power Sources. 2012;213:180–5. doi: 10.1016/j.jpowsour.2012.04.033.
[43] Chojnacka A, Świętosławski M, Maziarz W, Dziembaj R, Molenda M. An influence of carbon matrix origin on electrochemical behaviour of carbon-tin anode nanocomposites. Electrochim Acta. 2016;209:7–16. doi: 10.1016/j.electacta.2016.05.044.
[44] Chojnacka A, Molenda M, Bakierska M, Dziembaj R. Electrochemical performance of Sn/SnO_2 nanoparticles encapsulated in carbon matrix derived from plant polysaccharides. ECS Trans. 2015;64:165–71. doi: 10.1149/06422.0165ecst.